

FULL-SCALE CRASH TEST OF A CIVIL HELICOPTER AT JAXA

Hirokazu SHOJI*, Hiromitsu MIYAKI*, and Hiroshi MATSUMOTO**

* Japan Aerospace Exploration Agency, ** Mitsubishi Heavy Industries, Ltd.

Keywords: *Helicopter, Crashworthiness, Crash Test, and Crash Simulation*

Abstract

A Mitsubishi MH2000 prototype #2 helicopter was crash tested on February 25, 2004 at Aerospace Center Airdrome Branch of Japan Aerospace Exploration Agency (JAXA) as a cooperation research between JAXA and Mitsubishi Heavy Industries, Ltd. (MHI). This is the 2nd helicopter full-scale crash test in Japan. The test conditions was 7.5 m/s vertical and 9.6 m/s horizontal velocities on to concrete with 2.7° nose-up pitch. The test was conducted with crash trajectory determined by guided rail method. The helicopter was instrumented with accelerometers, strain gauges, and load cells. Photographic data was collected with video cameras and high-speed cameras as well. These crash data were collected to validate a computer simulation of the full-scale crash test. The simulation is performed with using a nonlinear, explicit transient dynamic finite element code LS-DYNA. In this paper, especially, results of structure acceleration responses are reported and then crash environment of seats are compared with airworthiness seat test conditions. Some accurate results of crash simulation with the current full-scale simulation model are described as well.

1 Introduction

In Japan, on crashworthiness research, the first crash test [1,2] was conducted by Kawasaki Heavy Industries, Ltd. (KHI) in 1985 with a BK117 helicopter. After that, KHI conducted research of subfloor structure members especially made of composite materials. And

from 1992 through 1995, research on subfloor structure members and aircraft seats at several manufactures were energetically conducted. In these days, several manufacturers research on helicopter subfloor structure members again. Whilst at JAXA and NAL (National Aerospace Laboratory in Japan, the former organization of JAXA), from 90's we researched on pipe-like shock absorbing devices and subscale aircraft underfloor model test and numerical simulation. After those we conducted vertical drop tests of YS-11 airliner fuselage sections in 2001 [3] and 2002 [4]. Further, we conducted a full-scale crash test [5] of a prototype of a Mitsubishi MH2000 helicopter at JAXA, on February 25th, 2004 as a cooperative research with MHI. This test is the second full-scale crash test of helicopter in Japan. The test had two major objectives. One was to acquire survival crash impact environment data, which were the impact response of airframe, seats, and anthropomorphic test dummies (ATD), of a civil helicopter which meets the requirements of the current airworthiness regulations. They would be reference data of a future crashworthiness improvement on helicopter, and of future airworthiness improvement on helicopter. In the test, crash trajectory determined by guided rail method was used to conduct crash testing. This test method has repeatability, makes easy to take high-speed camera pictures because the crash impact point is almost fixed, and is possible to conduct the test in relatively small area. This test was conducted by sliding the helicopter along the rail from a height of 9m, which would result in an impact velocity of 7.9 m/s vertical and 10.5 m/s horizontal velocities on to concrete with 4° nose-up pitch as a

simulated case of a landing failure after an autorotation mode. This test simulated a severe, but survivable, crash impact. The other objective of the test was to acquire validation data of actual helicopter analytical simulation model. Numerical simulation is indispensable to evaluate and design crashworthiness of aircraft structures, seats, and other equipments, because evaluating every structure and equipments by actual tests is impractical due to its cost and time. If we can make a numerical model which simulates the test accurately, we can simulate the crash test on other various test conditions. And we can evaluate the helicopter structure and modified underfloor structure with improving its shock absorbing ability. Therefore, we are aiming at attaining accurate simulation model evaluated by actual crash environmental data. In this research, an nonlinear explicit transient finite element code LS-DYNA, are used to simulate the crash test [6, 7].

In this paper, we explain the test method, mock-up test, acceleration results of the test, seat environment compared with seat regulations [8], and some results of numerical simulation with the current model.

2 Test Description

2.1 Test Article

The test article was the second prototype for flight tests of Mitsubishi MH2000 helicopter, as shown in Figure 1, which was developed by MHI. It was used for the test after its all planned flight tests had finished. The maximum gross mass of the prototype helicopter is 4,500 kg. The center of gravity was located at station 4,977 mm from the nose. Although the helicopter has 10 seats, two seats of them were removed for using as measurement space and eight seats of them was occupied by instrumented 50th percentile male Hybrid II anthropomorphic test dummies but only co-pilot seat was occupied by a 50th percentile male Hybrid III ATD. Some components, such as an engine, main rotors, tail rotors, a main rotor gear

box, a tail rotor gear box, some pilot apparatus and so on, were replaced dummy weights to adjust the center of gravity, total weight and moment of inertia of the test article to ones of the real prototype of the helicopter as accurately as possible. The fuel tank was filled with water to represent an almost full load of fuel. Figure 2 shows the replacement of the components.

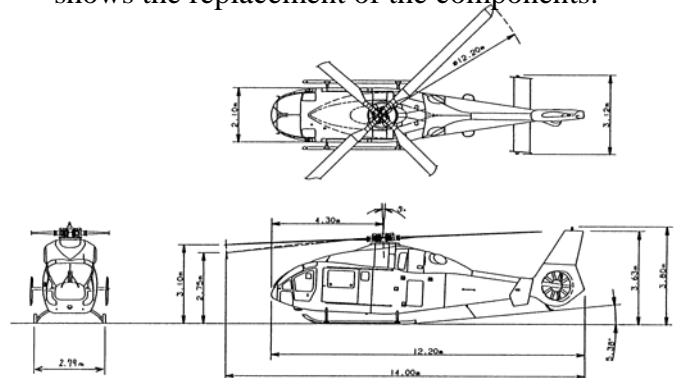


Fig. 1. The Second Prototype of Mitsubishi MH2000 Helicopter

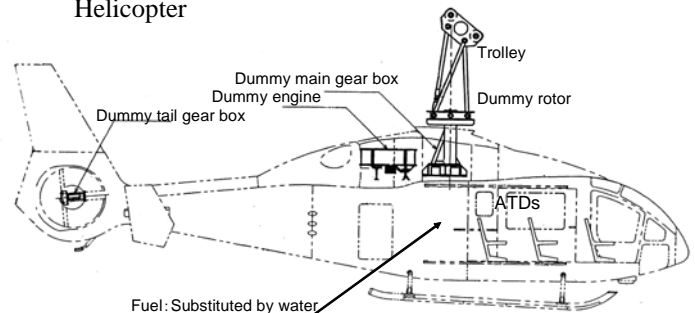


Fig. 2. Replacement of Components

2.2 Crash Trajectory Determined by Guided Rail Method

In this test, crash trajectory was determined by a guided rail. A gateway, which consists of two steel posts and a steel header, was built on the surface of the full-scale test hanger. A 22m long I-beam was suspended from the header of the gateway by one side to be free pitch direction rotating, and a crane by the other side. Suspension and release mechanism consists of a trolley, a release hook cart, and a winch on the ground. The trolley was equipped over the dummy rotor of the test specimen. The trolley and the release hook cart have rollers and can move smoothly up and down on the upper surface of the bottom flange of the I-beam. They connect through steel wires and a ring. The release hook captures the ring while its air

power actuator is non-pressure state and when the actuator is given air pressure, the hook releases the ring and the specimen slides down. The release hook connects to the winch on the ground through a pulley at the top of the beam by a steel wire. The specimen is set to the height of 9m, the test condition, by winding wire up by the winch. Reinforced concrete plates were spread all over the surface of crash test site in the hanger. And steel barriers were set the surrounding site. Figure 3 shows a schematic view of the test method. Figure 4 and 5 show the outside view of the test site and the inside one, respectively. This test method has repeatability and makes easy to take high-speed camera pictures because the crash impact point is almost fixed.

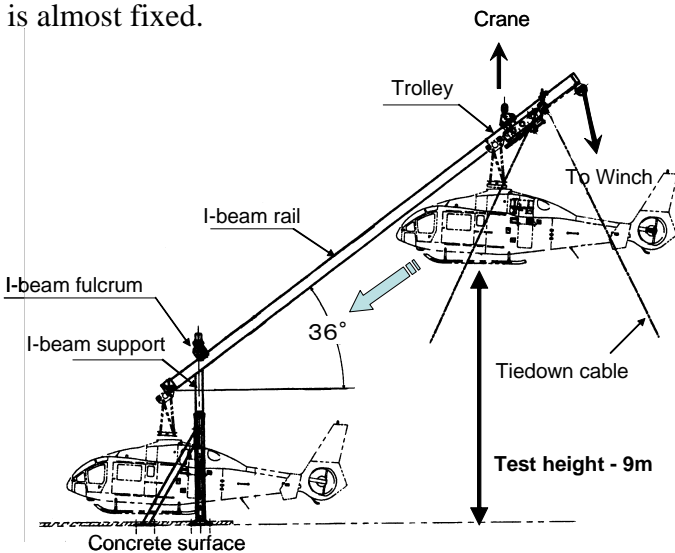


Fig.3. Schematic View of the Crash Trajectory Determined by Guided Rail Method



Fig. 4. Outside View of the Test Site



Fig. 5. Inside View of the Test Site

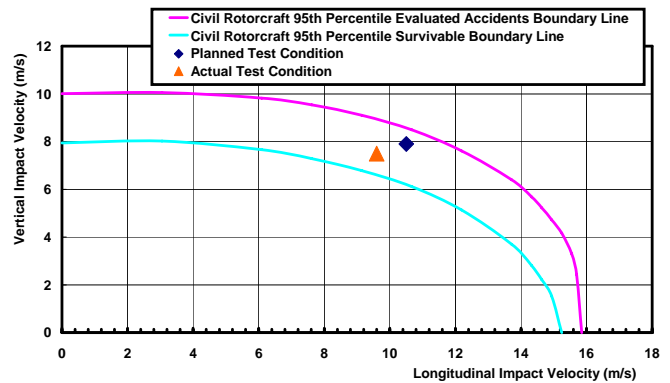


Fig. 6. Comparison the Test Condition with Impact Velocity Envelope

2.3 Test Impact Condition

The crash test impact conditions were determined as follows:

- The flight path angle: 37°.
- Longitudinal component of the impact velocity: 10.5 m/s.
- Vertical component of the impact velocity: 7.9 m/s.

So, the impact velocity is 13.2 m/s.

- Attitude of the specimen: pitch direction is nose-up +4°, yaw and roll directions are 0°.

The crash scenario was as follows. The helicopter starts autorotation at the maximum horizontal speed 18.5 m/s of unsafe area of high altitude portion of Height-Velocity Diagram of MH2000 helicopter, that is, the knee of the curve, sinking vertical speed of 14m/s, and the flight path angle of 37°. Then the helicopter kept autorotation flight at the same flight path angle with reducing its sink speed, but finally it failed to flare, and then it crashed to the ground with the same flight path angle. The vertical component of impact velocity is the vertical

component of the velocity of dynamic seating system test requirements because there is no dynamic structural regulation on civil helicopters. Figure 6 shows civil rotorcraft accidents survival limits of impact velocity and the test conditions [9]. It shows that the test condition was a severe but survival crash impact.

2.4 Instrumentation

Onboard instrumentation used to obtain data pertaining to the dynamic behavior of the helicopter structure, major components, ATDs, and seats included 140 accelerometers, 45 strain gages, 6 seat belt tension transducers. There were 3 data acquisition systems in the test. Two of them were on-board data acquisition systems, 128-channel KYOWA DIS-2000A system and 32-channel DIS-3000A system. Withstanding vibration of 100G applied for 10ms, 1000times in each triaxial direction is shock resistance ability of them. They were powered by internal battery. And the other data acquisition system as a back-up system of the on-board systems was used to collect data of 20 accelerometers and 12 strain gages. This one was equipped on the ground and connected to sensors by umbilical. All systems collected 10,000 data per second by 12-bit analogue-to-digital (A/D) converter simultaneously on each channel.

Four high-speed motion cameras were used to record the test. One external high-speed motion-picture camera was used to determine the impact velocity, while the others were used to record various views of the impact. Video cameras were also used to record the test. Six video cameras were located around the exterior of the airplane in order to capture a variety of views of the test.

The trigger signal is activated at the moment of pulling off a connection pin simultaneously the release hook releasing the connection ring due to opening the hook. The trigger signal transmitted to all acquisition systems and high-speed motion-picture cameras at the same moment.

2.5 Mock-up Test

Three times mock-up tests, from the height of 2m, 4m, and 5m, were conducted preliminarily for establishing the test procedures and confirming appropriation of the method of the crash test.

A mock-up test article, which was made of steel beams, was designed to adjust its external forms, total weights, center of gravity, and moment of inertia to ones of the test article as accurately as possible. Figure 7 shows a side view of the mock-up test article. In the figure, shaded picture is the mock-up test article and the MH2000 helicopter is depicted in layers in comparison. A veneer of its nose simulates the outline of the helicopter and veneers of its tail are equipped for evaluating effects of lateral winds during sliding down. Figure 8 is a picture of the article in release position of the third mock-up test

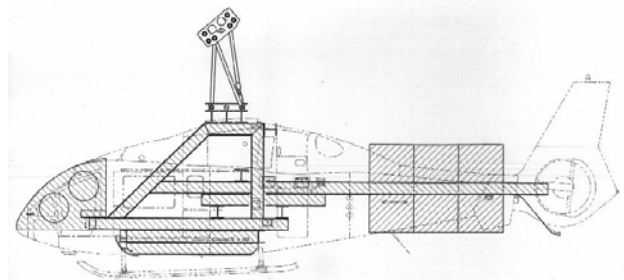


Fig. 7. A Side View of the Mock-up Test Article



Fig. 8. Mock-up Test Article in Release Position

3 Crash Test Results

3.1 Results of Impact Conditions

Table 1 shows the results of impact conditions with planned impact conditions for the 3rd preliminary mock-up test and the crash test. Error values and energy loss values were almost equivalent between two cases. Therefore, when

we set test height in the next crash test, we'll be able to acquire accurate impact condition by considering 14% energy loss. But, it is difficult to acquire accurate pitch angle because this method generates pitch moment after the hook releasing the trolley at the start of the test.

Table 1. Results of Impact Conditions

		Planned conditions	Crash conditions	Error (*)	Energy Loss
Mock-up Test	Horizontal Velocity (m/s)	7.3	6.7	-8.2%	
	Vertical Velocity (m/s)	6.8	6.4	-5.9%	
	Corresponding Velocity (m/s)	10	9.3	-7.1%	-14%
	Pitch Angle (°)	4.0	3.2	-0.8	
The Crash Test	Horizontal Velocity (m/s)	10.5	9.6	-8.6%	
	Vertical Velocity (m/s)	7.9	7.5	-5.1%	
	Corresponding Velocity (m/s)	13.1	12.2	-7.3%	-14%
	Pitch Angle (°)	4.0	2.7	-1.3	

Note(*): Definition of errors; velocity = (crash condition /planned condition)-1, and Angle=(crash)- (planned).

3.2 Results of Vertical Accelerations

Figure 9 shows results of the maximum acceleration values of the vertical direction on each measurement point with the stations of the sensors. And Figure 10 shows results of the duration time of the maximum acceleration from the contact moment of each sensor position with the station of the sensors. In these figures, L, R, FlrBot, SeatAtтч, CameraPL, SeatBack, SeatBackP, CG, TGB, AirCon, MGB, and EGN mean left-hand side and right-hand side on the same station, on the bottom of underfloor structure, on seat attachments, on the plate of setting on-board high speed video camera, on the center of the seat back, on the center of the pilot seat back, center of gravity, tail gear box, under the air conditioner, main gear box, and engine, respectively. And numbers in parentheses in the legend stand for height from the cabin floor in mm. From these figures, accelerations between the forward skid and the aft skid, that is the passenger cabin area,

are more moderate than near the skids. Naturally, the lower position was suffered the higher acceleration. The peak duration time of a station was the almost same on the same station except upper heavy devices equipped with moderately flexible structure and TGB. Figure 11 shows acceleration time history curves of some points with CFC60 [10]. In the figure, the time of zero is the moment of contact of the aft edge of the left skid to the concrete ground surface, and S5790LBU stands for the upper flange of left keel beam at the station 5790. From Figs. 10 and 11 show that upper portion acceleration responses and the lower portion acceleration responses occur at the same time around the same station. Therefore, when we

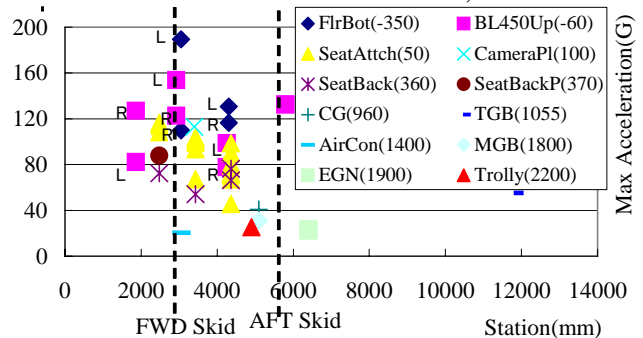


Fig. 9. Results of the Maximum Acceleration Values

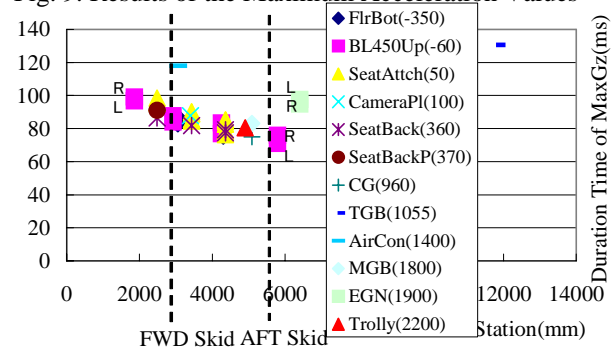


Fig. 10. results of the duration time of the maximum acceleration

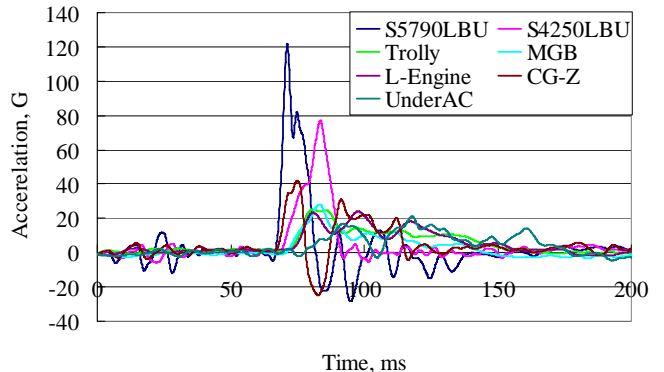


Fig. 11. Acceleration History Curves of Some Points

estimate cabin acceleration responses using numerical simulation, we have to consider effects of the upper portion structure, that is, we have to simulate with full-scale structure.

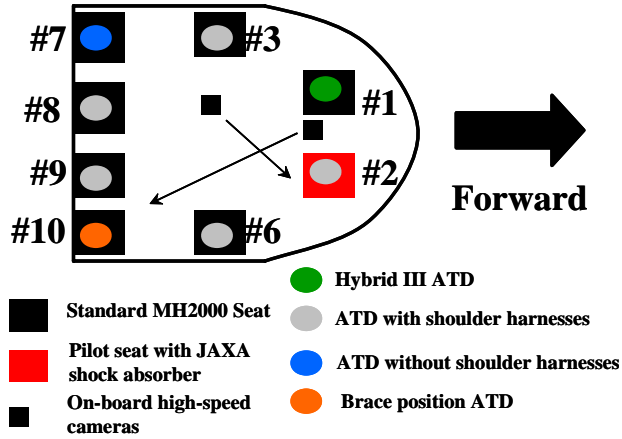


Fig. 12 Seat Arrangement in the Helicopter Cabin

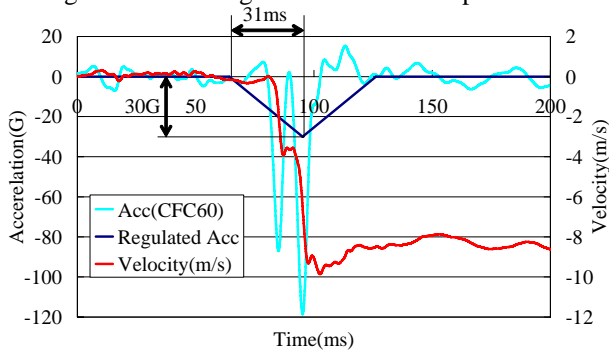


Fig. 13. Vertical Acceleration History of #1 Seat Attachment of Left Leg

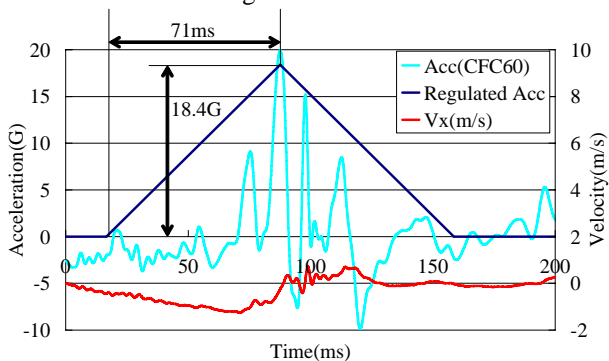


Fig. 14. Longitudinal Acceleration History of #1 Seat Attachment of Left Leg

3.3 Comparison between Test Results and FAR 29.562

In this test, the vertical component of impact velocity is the vertical component of the velocity of dynamic seating system test requirements. Therefore, we compare the test results with emergency landing dynamic

conditions, FAR 29.562. Although seats are declined from the axes with considering effects of floor warp or discrepancies between the maximum load direction and the landing direction in the regulation, we couldn't decline seats in the crash test, thus, we verify test results in the vertical direction and the longitudinal direction. Figure 12 shows seat arrangement of the helicopter cabin of the crash test. Figure 13 is an example of vertical acceleration history curve and velocity change. In the regulation, a change in downward velocity is not less than 30 feet per second (9.14m/s) and peak floor deceleration must occur in not more than 0.031 seconds after impact and must reach a minimum of 30g's. In the figure, ACC means acceleration. And Figure 14 is an example of longitudinal acceleration history curve and velocity change. In the regulation, a change in forward velocity is not less than 42 feet per second (12.8m/s) and peak floor deceleration must occur in not more than 0.071 seconds after impact and must reach a minimum of 18.4g's. The pilot seat, #2, was equipped with JAXA shock absorbing devices outside of the seat back like Figure 15 excluding the standard shock absorbing device, wire bending shock absorber from the seatback. The shock absorber didn't work well in the test. Because estimated load was too high to work the device, the seat frame broke and deformed, then the seat pan didn't slide. Therefore, the pilot seat is able to estimate as a seat without shock absorbing device. The ATD on #10 seat sat with brace position like Figure 16 without shoulder harness. The ATD on #7 seat sat without shoulder harness for comparison with #10. Table 2 is summary of seat acceleration and velocity change, seat strap loads, and ATD pelvis acceleration. We couldn't measure lumber loads of ATDs, therefore, we roughly estimated lumber load from the pelvis accelerations result. In the regulation, loads in individual shoulder harness straps must not exceed 1,750 pounds (7.78kN), if dual straps are used for retaining the upper torso, the total harness strap loads must not exceed 2,000 pounds (8.90kN), and the maximum compressive load measured between the pelvis and the lumber column of the ATD must not

exceed 1,500 pounds (6.67kN). But, we didn't measure lumber loads of ATDs, thus, we evaluate damage of dummies with Eiband curve [11] like Figure 17.



Fig. 15. JAXA Shock Absorbing Device Seat Fig. 16. Brace Position

Table 2. Summary of the Results of the Seats

	Regu.	#1	#2	#3	#6	#7	#8	#9	#10
L AZ(G)	30	134		75	115	86	95	88	73
L VZ(m/s)	9.14	9.85		8.9	8.2	7.7	7.6	9.3	8.0
L AX(G)	18.4	30		41		35	36	33	23
L VX(m/s)	12.8	2.0		3.2		2.7	2.6	2.7	2.5
R AZ(G)	30	132	124	123	117	102	93	77	57
R VZ(m/s)	9.14	9.7	9.4	8.8	7.4	8.2	8.3	7.9	7.9
R AX(G)	18.4	22	44	42	25	34	31	28	22
R VX(m/s)	12.8	2.4	2.5	2.6	2.3	3.0	2.5	2.3	2.7
DZ(G)		26	53	27		28	30	25	46
Splice(kN)	8.9					2.4	2.2	2.2	10.3
Seat Pan Displacement (mm)		201.7	51.2	115.1	116.4	110.0	70.0	102.6	30.1

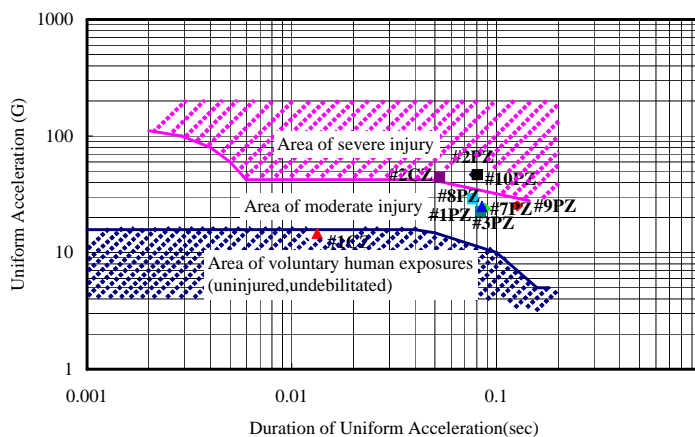


Fig. 17. Eiband Curve for the results of the seat

In Table 2, Regu. means regulation value, and L, R, D, A, V, Z, and X mean on the attachment of Left leg of the seat, on the attachment of Right

leg of the seat, dummy, acceleration, velocity, Z direction (vertical direction), and X direction (longitudinal direction), respectively. In Figure 17, P and C mean pelvis and chest, respectively. From Table 2 and Figure 17, seat impact environments were severe in vertical direction, but survival except #2 dummy, and we couldn't evaluate the results of #10 dummy because the pelvis Z-direction acceleration did not align to the vertical direction and its upper torso didn't hold with shoulder harness, so it was easy to move at the impact and shock absorbing device of #10 seat worked little. Therefore, harness load of #10 dummy was beyond the regulation value. #2 dummy was too severe to survive, because the #2 seat was the almost same as the non shock absorbing seat.

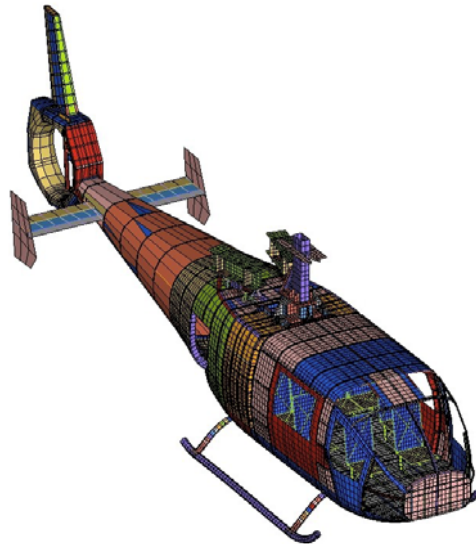


Fig. 18. Full-Scale Simulation Model as of now

4 Numerical Simulations

Figure 18 shows full-scale helicopter simulation model as of now with nonlinear explicit transient finite element code LS-DYNA. The simulation model was mainly modeled using shell elements, but TGB dummy and engine dummies were modeled with solid elements and those equipment components are modeled with beam elements. Fairing covers of the head part of the helicopter were replaced by lumped masses because the fairing wouldn't affect the behavior of the model. The components with heavy mass like the dummy weights of the main gear box, the engines, and the tail gear box and

like fuel tanks were adjusted configuration to simulate mass distribution as accurately as possible, unless they were replaced by lumped masses. We use fully integrated shell elements for the under floor structure to simulate actual twisting deformations, although we used Belytschko-Wong-Chiang type one-point quadrature element for the upper structure. Seats

weren't modeled its shock absorbing device, were only simulated their located positions and their mass. ATDs were replaced by lumped masses. The model has about 50,000 elements. Figure 19 shows the comparison of numerical simulated deformation with photographs from the high-speed film in sequential pictures.

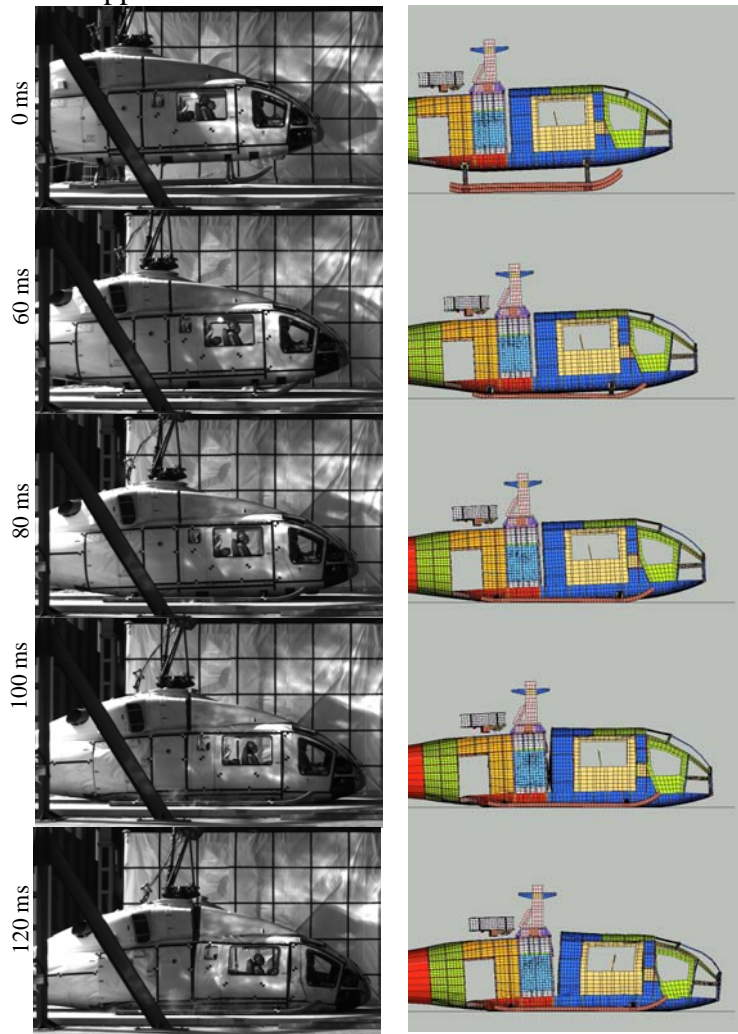


Fig. 19. Comparison of Simulated Deformation with Photographs from the High-Speed Film

Table 3. Estimated Sequences of Crash Events from the Test Results and the Simulation Results

Crash Event	Estimated Time (ms) by Test	Estimated Time (ms) by
The tail of the left skid touched the ground.	0	0
The tail of the right skid touched the ground	12-14	12
The forward part of the left skid touched the ground.	18-20	8
The forward part of the right skid touched the ground.	24-26	22
The aft portion of the bottom surface of the helicopter touched the ground.	70	70
The radar dome on the bottom forward surface of the article touched the ground.	86	88
The tail skid touched the ground.	90	92

Table 3 shows Estimated sequences of crash events from the test results and the simulation results. From Figure 19 and Table 2 show the simulation model expresses the gross behavior well. But the simulation model of the skid wasn't simulated well.

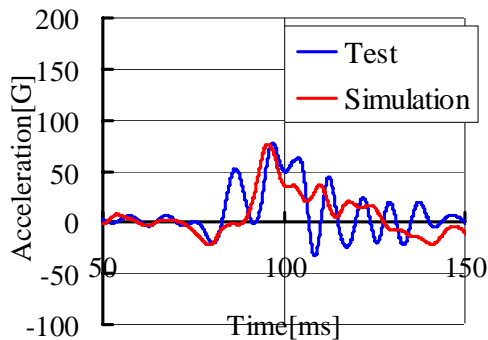


Fig.20 Accelerations on Left Keel Beam at Station 1860

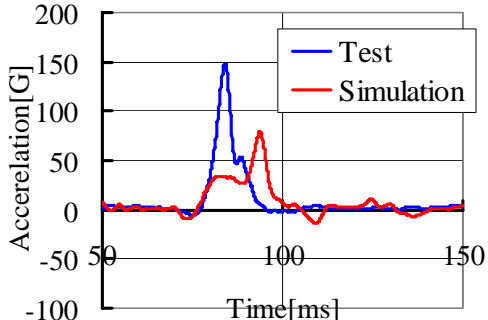


Fig.21. Accelerations on Left Keel Beam at Station 2920

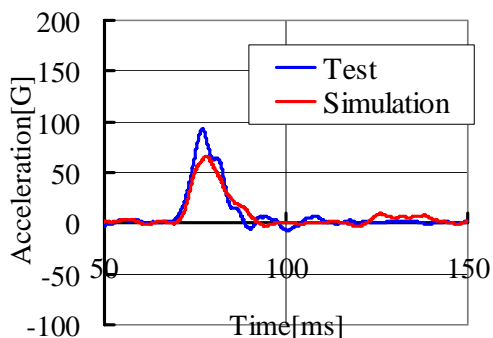


Fig.22. Accelerations on Left Keel Beam at Station 4250

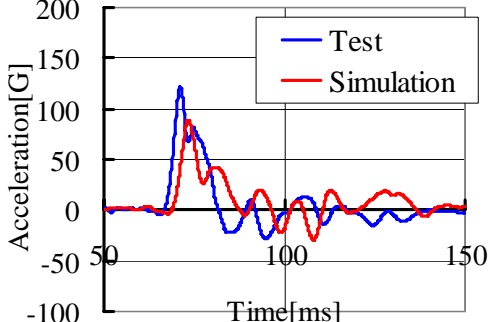


Fig.23. Accelerations on Left Keel Beam at Station 5790

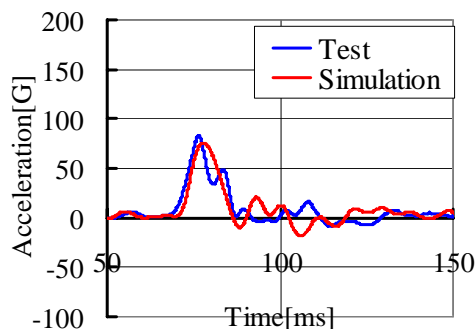


Fig. 24. Acceleration on the Attachment of Left Leg of 3rd Row Seat

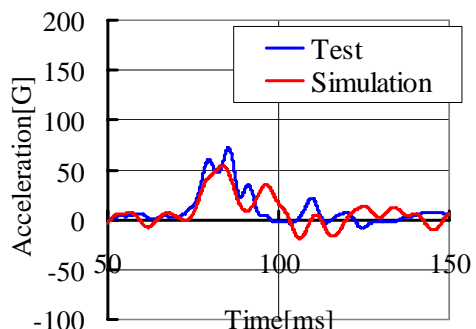


Fig. 25. Acceleration on the Attachment of Left Leg of 2nd Row Seat

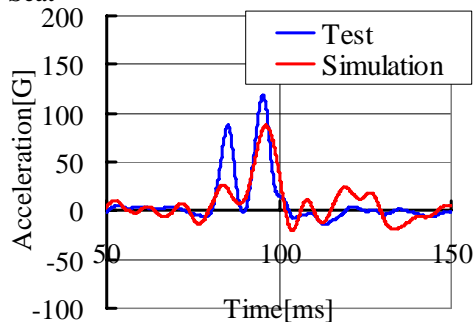


Fig. 26. Acceleration on the Attachment of Left Leg of Co-pilot Seat

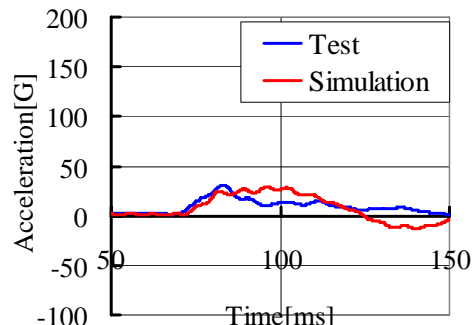


Fig. 27. Acceleration at Main Gear Box

From Figure 20 to Figure 27 show correlation results between the test and the simulation for vertical (Z) direction acceleration. The results have good correlation except Figures 20 and 21.

The station 2920 is near the location equipped with the forward skid. Therefore, the results were affected by the skid model. And the station 1860 is forward part of pilot cabin. Therefore, there is many kinds of control devices and balance weights in the part and it is difficult to acquire good correlations.

5 Concluding Remarks

We conducted a crash test of a helicopter successfully and could acquire test data of the real full-scale impact environment. And we showed we can also use those data as reference data for validation of a full-scale simulation model. With the test, we could show the availability of the crash trajectory determined by guided rail methods. The seat environment of the test was severe but survival, therefore the test condition was adequate. Simulation results showed good correlation between the test and the simulation. And gross behavior of the helicopter in the test was simulated on the whole.

We intend to evaluate gross structural deformations after the impact and effect of accelerations to the deformation. On the other hand, on simulation we intend to modify the model until it will be able to reproduce the crash test accurately. Modification of skid structure modeling, windshield modeling, ATDs modeling, seat modeling, and jack points modeling will be conducted as the next works.

Acknowledgement

This crash test couldn't be conducted without cooperation of many persons. The authors would like to thank Professor T. Ueda of Nagoya University and T. Kobayashi of MHI, for providing us the opportunity of the crash test. The authors also wish to thank K. Iwasaki, M. Minegishi, I. Kumakura, S. Machida, N. Yoshimoto, K. Takasaki of JAXA, K. Abe of MHI, T. Kuriki, S. Miura, K. Suzuki, I. Kikuya of Churyo Engineering and R. Kizaki of Shinko Construction Machinery for conducting the test with our cooperation. Appreciation is extended to K. Sakura, N. Higuchi, M. Toyama, Dr. K.

Togami, K. Ogino of MHI, M. Watanabe, S. Touchi, of Churyo Engineering for supporting the test and to F. Baba, A. Sassa, and M. Masuda, Ryoyu Systems Co., Inc. for their assistance during the finite element models development.

References

- [1] Och F. Crashworthiness activities on MBB helicopters, AGARD CP-443, 1988.
- [2] Ohnishi M. Yoshimura T and Hirano M. A crash test of a BK117 helicopter, Proceedings of the JSASS/JSME 27th Structures Conference, 1985, pp.300-303. (in Japanese)
- [3] Kumakura I, Minegishi M, Iwasaki K, Shoji H, Yoshimoto N, Terada H, Sashikuma H, Isoe A, Yamaoka T, Katayama N, Hayashi T, and Akaso T. Vertical drop test of a transport fuselage section, SAE Paper 2002-01-2997, Nov. 2002.
- [4] Kumakura I, Minegishi, M, Iwasaki K, Shoji H, Miyaki H, Yoshimoto N, Sashikuma H, Katayama N, Isoe A, Hayashi T, Yamaoka T, and Akas T. Summary of vertical drop test of YS-11 transport fuselage sections, SAE Paper 2003-01-3027, Sep. 2003.
- [5] Shoji H, Iwasaki K, Miyaki H, Minegishi M, Kumakura I, Yoshimoto N, Machida S, Takasaki K, Matsumoto H, and Abe K. A crash test of a civil Helicopter, Proceedings of the 42nd Aircraft Symposium, Paper 3B6, Tokyo, Oct. 2004. (in Japanese)
- [6] Shoji H, Miyaki H, Iwasaki K, Matsumoto H, Ogino K, and Abe K. A post crash test analysis of a civil helicopter with a FEM code, 5th International KRASH User's Seminar (IKUS5), session 4, Milan, Italy, Sep. 2005.
- [7] Miyaki H, Shoji H, Iwasaki K, Kumakura I, Minegishi M, Matsumoto H, Ogino K, and Abe K. A simulation of full-scale crash test of a civil helicopter with FEM code, International crashworthiness conference, ICRASH2006, 2006-69, Athens, Greece, Jul. 2006.
- [8] Title 14 Code of Federal Regulations, Part25, Amendment 29-41, Section 25.562, Emergency landing dynamic conditions, Published in Federal Register, Aug. 29 1997.
- [9] Soltis S J and Olcott J W. The development of dynamic performance standards for general aviation aircraft seats, SAE Paper 850853, 1985.
- [10] SAE, Surface Vehicle Recommended Practice, SAE-J211/1 (Revised March 1995)
- [11] Eiband A M. Human tolerance to rapidly applied accelerations: a summary of the literature, NASA Memorandum 5-19-59E, June 1959.